Available online at www.sciencedirect.com

SCIENCE DIRECT®

Thin Solid Films 478 (2005) 96–102

thin solid films

www.elsevier.com/locate/tsf

# Characterization of spray deposited bismuth oxide thin films and their thermal conversion to bismuth silicate

O. Rico-Fuentes[a], E. Sánchez-Aguilera[b], C. Velasquez[c], R. Ortega-Alvarado[d], J.C. Alonso[a], A. Ortiz[a,*]

[a]*Instituto de Investigaciones en Materiales, UNAM. A. P. 70-360, Coyoacán 04510, D. F., México*
[b]*Departamento de Física Y Matemáticas, Universidad Iberoamericana Prol. P. de la Reforma 880, Álvaro Obregón 01210, D. F., México*
[c]*Departamento de Química, Universidad Autónoma Metropolitana A. P. 55-534, Iztapalapa 09340, D. F., México*
[d]*Facultad de Ciencias, UNAM. A. P. 70542, Coyoacán 04510, D. F., México*

Received 12 February 2004; received in revised form 24 August 2004; accepted 14 October 2004
Available online 18 November 2004

**Abstract**

Bismuth oxide films deposited by spray pyrolysis, using bismuth acetate or bismuth chloride, onto clear fused quartz and single-crystalline silicon substrates were thermally converted into bismuth silicate compounds. Bismuth silicate compounds' chemical compositions depend on the annealing temperature; $Bi_2SiO_5$ is obtained at 600 °C and $Bi_4Si_3O_{12}$ is produced at 750 °C. Forbidden energy optical band gap increases from 3.78 eV for as-deposited films up to 4.89 eV for annealed films. Current densities of $10^{-6}$ A/cm$^2$, in metal-insulator-semiconductor (MIS) structures, are observed for $Bi_2SiO_5$ films at applied electric fields 300 kV/cm and for $Bi_4Si_3O_{12}$ films for 2.5 MV/cm. A value of the order of 10.6 was calculated for the apparent dielectric constant of the specimen obtained by annealing at 800 °C.


*PACS:* 73.61.N; 77.55; 82.30.L; 77.84.B
*Theme:* Synthesis
*Topic:* Characterization
*Keywords:* Insulators; Dielectric properties; Pyrolysis; Oxides

## 1. Introduction

Bismuth oxide and bismuth silicate are interesting materials due to their optical and electrical properties, which confer them a wide variety of potential applications. Among other properties, bismuth oxide ($Bi_2O_3$) has large energy band gap, refractive index, dielectric permittivity and photoconductivity [1]. All these characteristics make bismuth oxide suitable for several applications, such as: gas sensors, optical coatings, photovoltaic cells, microwave integrated circuits and as an oxygen conductive electrolyte in electrochemical cells [2,3]. $Bi_2O_3$ shows polymorphism with four main modifications that are known as α-, β-, γ-, and δ-$Bi_2O_3$. These modifications possess different crystalline structures, electrical and optical properties. The α and δ phases are stable and the β phase and γ phase are metastable. Bismuth oxide thin films have been prepared by several methods, such as: anodic and thermal oxidation of bismuth films, reactive activated evaporation, rf sputtering, hydrothermal processes, laser ablation, etc. [4–7]. From a structural point of view, bismuth silicate shows, besides of amorphous phase, three crystalline phases with different chemical composition, such as: $Bi_{12}SiO_{20}$, $Bi_2SiO_5$ and $Bi_4Si_3O_{12}$. Crystalline $Bi_{12}SiO_{20}$ is a nonferroelectric photorrefractive material, which has a strong optical activity and has potential applications as active element in optically addressed two-dimensional spatial light modulators, real-time holography and optical phase conjugation [7]. $Bi_2SiO_5$

* Corresponding author. Tel.: +52 56224599; fax: +52 56161251.
*E-mail address:* aortiz@servidor.unam.mx (A. Ortiz).

0040-6090/$ - see front matter © 2004 Elsevier B.V. All rights reserved.
doi:10.1016/j.tsf.2004.10.013

is a material with relatively good dielectric properties; besides, it has shown pyroelectric and nonlinear optical effects. Its non-centrosymmetrical crystalline structure may cause ferroelectric effect [8]. $Bi_4Si_3O_{12}$ is considered as a good replacement for bismuth germanate in scintillation detectors due to its physical properties, such as melting point, density, optical and scintillation characteristics and refractive index [9].

All these compounds can be obtained by mixing $Bi_2O_3$ and $SiO_2$ in suitable molar ratios. It is known that a silicon oxide layer, called native oxide, is formed on single-crystalline silicon substrates when they are exposed to atmospheric conditions. It has been reported that a silicon dioxide layer is developed when metallic oxides are deposited onto naked silicon substrates by the spray pyrolysis process [10]. On the other hand, for production of dynamic random access memory and ferroelectric non-volatile random access memory, it is required to deposit a dielectric thin film with a high dielectric constant and with ferroelectricity on silicon wafers [11]. There are scarce reports on the preparation and characterization of bismuth silicate films on silicon wafers.

In this work, we report the deposition of bismuth oxide films onto (100) silicon substrates, its thermal transformation to bismuth silicate compounds and their characterization.

## 2. Experiment

Bismuth oxide thin films were deposited by the pneumatic version of the spray pyrolysis process using bismuth acetate or bismuth chloride as bismuth source materials [12]. The spraying solutions were 0.1 M of bismuth acetate dissolved in pure methyl alcohol. The films were deposited at a substrate temperature of 450 °C. The solution flow rate and the gas flow rate were kept constant at 12.5 $cm^3$/min and 10 l/min, respectively. Some of the films prepared on both quartz and silicon single-crystalline slices were annealed for 2 h in air at the following temperatures: 500, 600, 650, 700, 750 and 800 °C. For X-ray diffraction and optical measurements, bismuth oxide films were deposited onto clear fused quartz slices. Meanwhile, for ellipsometry and infrared spectroscopy measurements, the substrates were n-type (100) silicon single-crystalline slices with electrical resistivity of 200 Ωcm. The native silicon oxide layer on the silicon substrate was removed by chemical etch with P solution (15 ml HF, 10 ml $HNO_3$ and 300 ml $H_2O$). The electrical integrity of the bismuth silicate films formed was analyzed by means of current–voltage (I–V) and capacitance–voltage (C–V) measurements on metal-insulator-semiconductor (MIS) devices, in which the dielectric films produced at 650 and 800 °C were incorporated. For these measurements, bismuth oxide layers were deposited onto n-type (100) silicon single-crystalline slices with 0.2 Ωcm, without native silicon oxide layer. The metallic electrodes onto the insulator layer were small discs of aluminium deposited by vacuum thermal evaporation with diameter of 1.0 mm. After removing the native oxide onto the back surface of the substrate, an indium–gallium alloy was used to make an electric contact. The crystalline structure of as-prepared and thermally converted films was analyzed by X-ray diffraction measurements achieved with a Siemens D5000 diffractometer, using the $CuK_{\alpha 1}$ radiation with a wavelength of 1.54050 A. The refractive index ($n$) and thickness of the films were measured with a Gaertner L117 ellipsometer using the 632-nm line from a He–Ne laser. The optical transmission and reflection spectra were recorded with a double beam UNICAM 260 spectrophotometer, with air in the reference beam. The infrared spectra were obtained with a Nicolet 5X FTIR spectrophotometer with a resolution of 4 $cm^{-1}$. The I–V and C–V characteristics were measured with automated systems. For the I–V measurements, a logarithmic picoammeter Keithley 1485 and a programmable voltage source Keithley 230, both coupled to a personal computer (PC) were used. Meanwhile, for C–V measurements, the automated system used is formed by a Keithley 230 programmable voltage source, Keithley 5951 remote input coupler and a Keithley 590 CV analyzer, coupled to a PC.

## 3. Results and discussion

Fig. 1 shows the X-ray diffraction spectra for an as-deposited bismuth oxide film prepared with bismuth acetate (Fig. 1A) and for samples annealed 600 °C (Fig. 1B), 700 °C (Fig. 1C) and 750 °C (Fig. 1D), respectively. Spectrum 1a shows well defined peaks associated with the $Bi_2O_{2.33}$ [13] and with the β-$Bi_2O_3$ [14] phases. The existence of the $Bi_2O_{2.33}$ phase indicates that the oxidation process is not

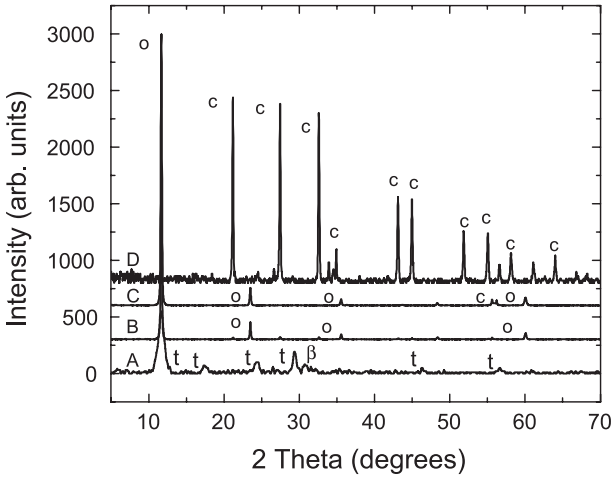


Fig. 1. X-ray diffraction patterns of (A) as-deposited bismuth oxide film and for films annealed in air at 600 °C (B), 700 °C (C) and 750 °C (D) for 2 hrs. The letters t, β, o and c mean the tetragonal, beta, orthorhombic and cubic phases, respectively.

complete. This spectrum indicates that the deposited material is formed by two bismuth oxide phases in separated grains. When the samples are annealed at 500 °C, the X-ray diffraction spectrum shows peaks associated with the orthorhombic $Bi_2SiO_5$ [15] phase and two peaks located at 27.6° and 55.5° related with the β-$Bi_2O_3$ phase. X-ray diffraction spectrum for sample annealed at temperature of 600 °C only shows peaks associated with the $Bi_2SiO_5$. The spectrum obtained for the sample annealed at 700 °C shows peaks related with the $Bi_2SiO_5$ phase and well-defined peaks related with the cubic $Bi_4Si_3O_{12}$ [16] phase. Furthermore, the spectrum obtained for the sample annealed at 750 °C corresponds to the $Bi_4Si_3O_{12}$ phase. Similar results were obtained for films deposited onto crystalline silicon slices.

The chemical composition of the identified material, by X-ray diffraction measurements, forming the films at different steps of annealing process can be explained if it is considered that during deposition at 450 °C, the decomposition of the bismuth acetate molecules is achieved and the atomic bismuth radicals, impinging on the surface of substrates, start to oxidize forming bismuth oxide. This process allows a bismuth oxide layer to be formed at that deposition temperature. In these conditions, a finite bismuth oxide source has been established. Besides, in parallel with this, an oxidation of the silicon surface exposed to the oxidizing ambient occurs. The evolution of chemical composition, due to annealing, can be explained in terms of an interdiffusion process between the bismuth oxide and the silicon oxide layers. The deposited film goes from a bismuth oxide chemical composition through a material with $Bi_2SiO_5$ phase up to another bismuth silicate compound with chemical composition corresponding to $Bi_4Si_3O_{12}$ phase. In this evolution, the bismuth/silicon ratio takes values of 2.00 and 1.33, respectively. These values indicate a trend toward a depletion of the bismuth source. On the other hand, it is observed that once the bismuth oxide is deposited, the annealing process permits to control the produced bismuth silicate compound, without the necessity of previous deposition of a silicon dioxide film. The thermal conversion of bismuth oxide films toward bismuth silicate films is possible, because, in all the substrates used, a silicon oxide film ever exists during bismuth oxide deposition and during the thermal annealing process.

From the ellipsometry measurements, the thickness and refractive index were calculated. The thickness of the as-deposited films takes different values ranging from 60 up to 76 nm, approximately, depending on the position of the substrate in reference to the arriving spray. After annealing, the thickness of the bismuth silicate films produced is increased, ranging from 69 up to 90 nm. These values depend on the annealing temperature, with the lowest value for films annealed at 500 °C and the highest value for films annealed at 800 °C. The increase in the thickness of the films is explained by the interdiffusion process between the deposited films and the silicon dioxide surface layer on the substrates. During formation of bismuth silicate compounds, silicon dioxide is incorporated in those films with the consequent augmentation in the thickness of the annealed films. Fig. 2 shows the variation of the refractive index as a function of the annealing temperature. Initially, it can be observed that the $n$ value decreases in the sample annealed at 500 °C. At that temperature, the formation of bismuth silicate starts. It is known that the silicon dioxide has a value of refractive index of about 1.46, then when the bismuth silicate compound is formed, the refractive index is decreased in proportion to the silicon dioxide layer that was formed. However, a silicon dioxide layer is always forming by oxygen diffusion through the bismuth oxide layer. For 600 and 650 °C annealing temperatures, the $Bi_2SiO_5$ compound is formed; the refractive index value increases because the silicon dioxide layer is being consumed and probably there is also a densification process of the formed silicate compound resulting in higher $n$ values. The refractive index shows a slight decrease for the sample annealed at 700 °C; in this case, as is shown by the X-ray diffraction results, the formed material is composed by a mixture of bismuth silicate compounds, $Bi_2SiO_5$ and $Bi_4Si_3O_{12}$. The lower $n$ value is due to formation of $Bi_4Si_3O_{12}$ phase. In samples annealed at 750 and 800 °C, the formed material is $Bi_4Si_3O_{12}$ phase; because this phase has a lower bismuth relative concentration, the value of the refractive index decreases.

Fig. 3 shows the infrared spectra for an as-deposited sample (Fig. 3a), for samples annealed at 500 °C (Fig. 3b) and 800 °C (Fig. 3c), respectively. In the spectrum for the as-deposited sample, there are peaks located at 462 and 1069 $cm^{-1}$ which are associated with the rocking and the stretching vibration mode of Si–O bond [17]. This fact indicates that a thin $SiO_2$ layer is developed at the interface between the deposited film and the silicon substrate. The peak located at 630 $cm^{-1}$ can be related to vibration of the Bi–O bond in stoichiometric compound. To our best knowledge, it is not possible to associate the well-defined peak located at 415 $cm^{-1}$ with some vibration mode of Bi–

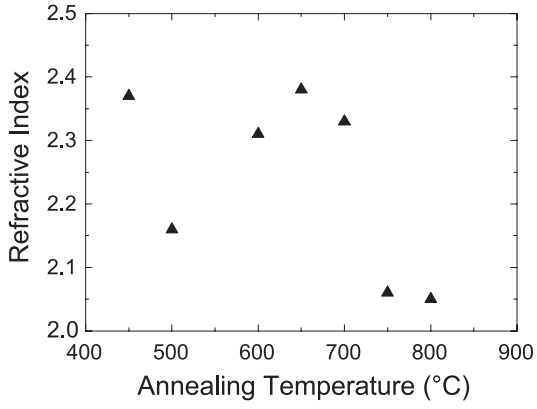


Fig. 2. Variation of the refractive index for bismuth oxide films deposited onto crystalline silicon substrates as a function of annealing temperature.

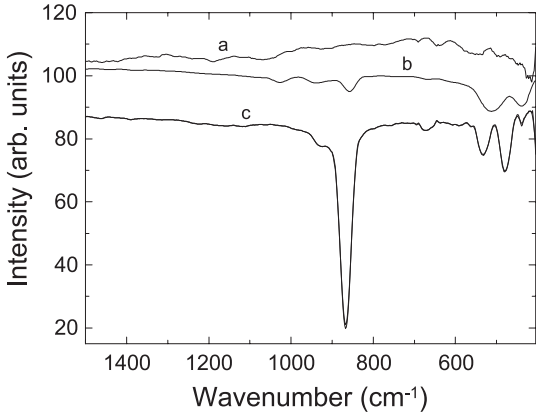


Fig. 3. FTIR spectra for an as-deposited bismuth oxide film (a) and for annealed films at 500 °C (b) and at 800 °C (c), corresponding to bismuth silicate compounds.

O bond. However, it could be associated with some vibration mode of the Bi–O bond in the oxide with chemical composition $Bi_2O_{2.33}$. The spectrum of Fig. 3b shows well-defined peaks located at 1011, 952, 863, 769, 699, 582, 485 and 435 $cm^{-1}$. The peak located at 1011 is related with the stretching vibration mode of the Si–O bond. The localization of this peak is shifted from that shown if Fig. 3a, due to the shift of this peak from 1070 for $SiO_2$ up to 940 for SiO. Although a thin layer of $SiO_2$ is developed at the interface between the substrate and the deposited film, the chemical composition of this silicon oxide layer changes by effect of diffusion on bismuth which reduced the oxide layer. The peaks located at 952, 863 and 769 $cm^{-1}$ are related with stretching vibration modes of $(SiO_4)^{4-}$ groups isolated from one another and forming a distorted tetrahedron. The peak located at 582 $cm^{-1}$ is associated with the bending vibration mode of distorted tetrahedron formed by $(SiO_4)^{4-}$groups. The absorption bands located at 485 and 435 $cm^{-1}$ are associated with absorption by $[BiO_6]$ polyhedron [18–20]. It is not possible to relate the peak located at 699 $cm^{-1}$ with a given vibration mode of some bond in the produced material.

The FTIR spectrum of Fig. 3c shows well-defined peaks located at 932, 870, 533 and 482 $cm^{-1}$. The peak located at 870 $cm^{-1}$ is due to absorption by the stretching vibration mode of Bi–O–Si bonds. This peak should be located at 880 $cm^{-1}$, but its position shows a blue shift when the bismuth content decreases in the $Bi_4Si_3O_{12}$ compound [20]. If this band and that located at 932 $cm^{-1}$ are considered, they have a similar form with those bands located at 1070 $cm^{-1}$ and the shoulder at 1190 $cm^{-1}$ observed in stoichimetric silicon dioxide. In that case, both absorptions are related with stretching vibration modes of Si–O–Si bond, one of them with vibrations of Si–O bonds in phase and the other one with vibration out of phase by $\pi$ [21]. In the present case, in the Bi–O–Si bonds, when the vibrations of the Bi–O and Si–O are in phase, the absorption is located at 871 $cm^{-1}$; meanwhile, if the vibrations are out of phase by $\pi$, the absorption band is located at 932 $cm^{-1}$. The shift observed in the bands location can be associated with the difference between the atomic masses of silicon and bismuth atoms. The band located at 533 is assigned to deformation vibration of isolated $(SiO_4)^{4-}$ groups forming distorted tetrahedron. The absorption band located at 482 $cm^{-1}$ is related with absorption by $[BiO_6]$ polyhedron. The FTIR spectra of Fig. 3 are in agreement with the X-ray diffraction results; there is an interdiffusion process between the bismuth oxide film and the silicon dioxide on the surface of the substrate resulting in the conversion of these metallic oxides into bismuth silicate layers with chemical composition depending on the annealing temperature. It should be remarked that a visible absorption band located at around 1070 $cm^{-1}$ is observed in the FTIR spectra for all the analyzed films, indicating that a silicon dioxide layer exists in the interface between the generated bismuth silicate film and the single-crystalline silicon substrate.

From the optical transmission and reflection spectra, considering various interfaces, the absorption coefficient ($\alpha$) was calculated taking into account the relation:

$$T = \frac{(1-R^2)\exp(-\alpha d)}{1-R^2\exp(-2\alpha d)} \quad (1)$$

$T$ and $R$ denote the transmission and reflection values, respectively, and $d$ is film thickness.

From Eq. (1), an expression for $\alpha$ is derived:

$$\alpha = \frac{1}{d}\ln\left\{\left[\frac{(1-R)^2}{2T}\right] + \frac{1}{\sqrt{\left[\frac{(1-R)^2}{2T}\right]^2 + R^2}}\right\}. \quad (2)$$

Taking into account that bismuth oxide and bismuth silicate are considered as direct energy band gap materials, Fig. 4 shows the $(\alpha h\upsilon)^2$ graph as a function of the photon energy ($h\upsilon$) for an as-deposited sample (Fig. 4a) and for samples annealed at 600 °C (Fig. 4b) and 750 °C (Fig. 4c),

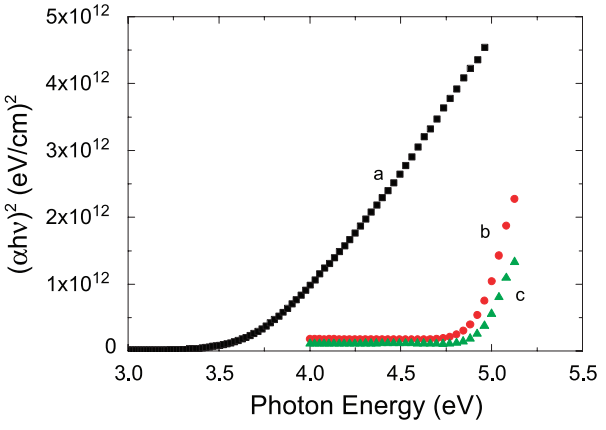


Fig. 4. $(\alpha h\upsilon)^2$ as a function of the photon energy for an as-deposited sample (a) and for samples annealed at 600 °C (b) and 750 °C (c). Considering allowed direct electronic transitions.

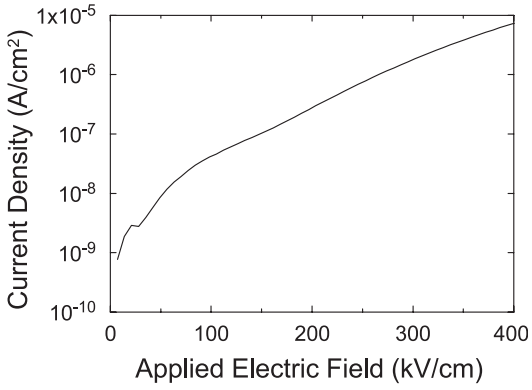


Fig. 5. Current density–applied electric field characteristics of a MIS structure incorporating a $Bi_2SiO_5$ insulating layer.

which are formed by $Bi_2SiO_5$ and $Bi_4Si_3O_{12}$, respectively. The calculated energy band gap (Eg) goes from 3.78 eV for the as-deposited film, to 4.80 eV for the sample annealed at 600 °C up to 4.89 eV for the sample annealed at 750 °C. This variation of the energy band gap is explained by the material formed during the annealing process, with the band gap acquiring higher values when bismuth silicates are produced. The increment in the Eg value is associated with the interdiffusion between the bismuth oxide, lower Eg value and silicon dioxide, which has an energy band gap of the order of 8.2 eV. It should be remarked that the energy band gap calculated for the as-deposited film, formed mainly by $Bi_2O_{2.33}$ and β-$Bi_2O_3$ phases, does not correspond to reported values for films formed only by β-$Bi_2O_3$ phase, of the order of 2.58 eV [22]. It has been reported that in bismuth oxide films, the phase composition of the analyzed material has a strong effect on its energy gap. For films with mixture of phases, with BiO phase as the predominant one over the α-$Bi_2O_3$ phase, the energy gap observed shows values of the order of 3.31 eV. This value is associated with the BiO phase, which has higher energy gap than that of the α-$Bi_2O_3$ phase (≈3.05 eV) [1]. In the present case, the X-ray diffraction results do not show any signal that can be associated with the existence of the BiO phase. This result permits us to infer that the high value calculated in this work for the as-deposited films could be related with the existence of the $Bi_2O_{2.33}$ phase in the deposited film.

Similarly, the calculated energy gap values for the annealed samples are higher than those reported values for single-crystalline samples of the $Bi_4Si_3O_{12}$. Optical transmission measurements on specimens with thickness of 22 mm show an absorption edge located at around 290 nm. This wavelength corresponds to photon energy of the order of 4.3 eV. The difference in the absorption edge is explained if it is considered the polycrystalline nature of the samples and their small thickness, in the present work. The absorption edge is shifted toward longer wavelength (≈303 nm) for specimens with higher thickness (188 mm). This shift is attributed to internal attenuation and to scattering in local surface quality [23]. Given the very small thickness of the films produced, in the present work, the internal attenuation effects should be strongly reduced.

The electrical integrity of the films produced incorporated in MIS structures was evaluated through current–voltage and capacitance–voltage measurements. Fig. 5 shows the current–voltage characteristics corresponding to films produced by means of an annealing treatment at 650 °C. In this figure, a displacement current density of the order of $10^{-9}$ A/cm$^2$ is observed for low applied electric fields, which is associated with the applied ramp voltage. The general form of the curve appears to indicate that large charge trapping effects exist, which are related with charge trapping in the volume of the film, without premature injection. When the electronic current is flowing through the bismuth silicate film, electrons are captured into deep traps. It is possible to observe that at different electric field regions, the curve shows several charge trapping ledges. This fact could indicate that charge traps are located at different energies. On the other side, dielectric breakdown is not observed for the highest applied electric field used in these measurements, although the current density is too high for those electric fields.

Fig. 6 shows the current density versus applied electric field characteristics of the $Bi_4Si_3O_{12}$ generated film. For applied electric fields lower than 0.5 MV/cm, there is a current density of the order of $10^{-8}$ A/cm$^2$, which can be related to the displacement current due to ramped applied voltage and to premature current injection due to stoichiometric deviations with metallic atoms in excess near the interface. For higher applied electric fields, the curve shows a charge trapping ledge. The charge is trapped in the volume of the bismuth silicate. However, there is not a dielectric breakdown for applied electric fields up to 3 MV/cm. It should be remarked that the maximum value for the current density is of the order of $10^{-6}$ A/cm$^2$, which is an acceptable value for a good insulating material. This behavior might be associated with the existence of a silicon dioxide layer at the interface between the bismuth silicate film and the substrate, as it is observed from the infrared

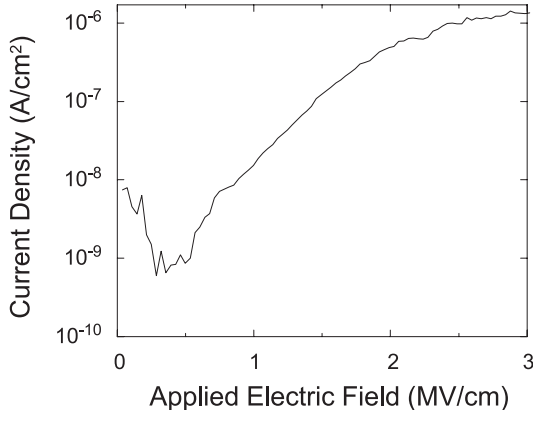


Fig. 6. Current density-applied electric field characteristics of a MIS structure, with $Bi_4Si_3O_{12}$ insulating layer.

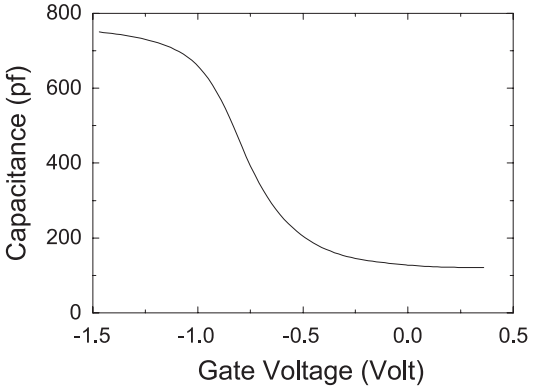


Fig. 7. High frequency capacitance-voltage characteristics of a MIS structure with $Bi_4Si_3O_{12}$ insulating layer.

spectra. The results for both bismuth silicate compounds are similar to those previously reported when they were incorporated in MIS structures [24,25].

The high-frequency capacitance–voltage characteristics for a MIS structure incorporating a 98-nm-thick bismuth silicate film produced by annealing at 800 °C are shown in Fig. 7. This curve shows a slight stretching effect along the voltage axis due to charge traps located at the interface. On the other hand, this curve is shifted toward negative gate voltage, indicating the existence of positive fixed charge in volume of the bismuth silicate. From the highest capacitance value measured, taking it as in accumulation condition, an estimated value of the order of 10.6 for the relative or apparent dielectric constant was obtained. The apparent dielectric constant value estimated in this work is in agreement with that previously reported for a MIS structure formed for a bismuth oxide layer deposited by metal organic chemical vapor deposition on a 100-nm $SiO_2$ layer thermally grown on a single-crystalline silicon wafer annealed at 780 °C by 30 min in nitrogen atmosphere, where the relative or apparent dielectric constant value is due to a low dielectric constant layer $\epsilon_l$ (silicon oxide) with thickness $d_l$, in series with a high dielectric constant layer $\epsilon_h$ (bismuth silicate) with thickness of $d_h$, as a double-layer capacitor. In the present work, we do not know the thickness of the low dielectric constant layer; however, if it is assumed that this layer is silicon dioxide with a dielectric constant of about 4, then the dielectric constant of the bismuth silicate layer produced by diffusion should have a dielectric constant value of the order of that reported [25].

## 4. Conclusions

Crystalline $Bi_2SiO_5$ and $Bi_4Si_3O_{12}$ films were obtained by air annealing bismuth oxide layers deposited by spray pyrolysis onto clear fused quartz and single-crystalline silicon slices at temperatures of the order of 600 and 750 °C, respectively. For a bismuth oxide film, its thermal conversion to bismuth silicate compounds is explained by a diffusion process. The refractive index has values ranging from 2.08 up to 2.37, depending on the obtained compound. Infrared spectra show absorption bands corresponding to the above mentioned bismuth silicate compounds. From optical transmission and reflection measurements, considering allowed direct electronic transitions, the energy band gap varies from 3.78 eV for as-deposited films to 4.80 eV for $Bi_2SiO_5$ and to 4.89 eV for $Bi_4Si_3O_{12}$ films. The current density-applied electric field characteristics show that current densities of $10^{-6}$ A/cm$^2$ through the specimens incorporated in MIS structures are observed for applied electric fields 300 KV/cm and 2.5 MV/cm, respectively. The apparent dielectric constant value of 10.6 was calculated from the capacitance–voltage characteristics for specimen annealed at 800 °C.

## Acknowledgements

The authors want to thank Dr. Aaron Sánchez for optical measurements and L. Baños and S. Jimenez for technical assistance. We also want to thank the partial support by CONACyT (México) and DGAPA-UNAM.

## References

[1] L. Leontie, M. Caraman, M. Delibas, G.I. Rusu, Mater. Res. Bull. 36 (2001) 1629.
[2] G. Bandoli, D. Barecca, E. Brescacin, G.A. Rizzi, E. Tondello, Chem. Vap. Depos. 2 (1996) 238.
[3] T. Hyodo, E. Kanazawa, Y. Takao, Y. Shimizu, M. Egashira, Electrochemistry 68 (2000) 24.
[4] J. George, B. Pradeep, R.J. Joseph, Thin Solid Films 148 (1987) 181.
[5] Q. Yang, Y. Li, Q. Yin, P. Wang, Y.B. Cheng, Mater. Lett. 55 (2002) 46.
[6] L. Armelao, P. Colombo, M. Fabricio, J. Sol–Gel Sci. Technol. 13 (1998) 213.
[7] J.C. Alonso, R. Diamant, E. Haro-Poniatowski, M. Fernandez-Guasti, G. Muñoz, M. Jouanne, J.F. Morhange, Appl. Surf. Sci. 109 (1997) 359.
[8] I. Koiwa, T. Kanehara, J. Mita, T. Iwabuchi, T. Osaka, S. Ono, M. Maeda, Jpn. J. Appl. Phys. 35 (1996) 4946.
[9] J.H. Kim, T. Tsumuri, H. Hirano, T. Kamiya, N. Mizutani, M. Daimon, Jpn. J. Appl. Phys. 32 (1993) 135.
[10] L. Castañeda, J.C. Alonso, A. Ortiz, E. Andrade, J.M. Saniger, J.G. Bañuelos, Mater. Chem. Phys. 77 (2002) 938.
[11] F. Scout, D.A. Paz de Araujo, Science 246 (1989) 1400.
[12] J. Aranovich, A. Ortiz, R.H. Bube, J. Vac. Sci. Technol. 20 (1979) 994.
[13] Powder Diffraction File, Joint Committee on Powder Diffraction Standards, ASTM, Newtown Square, PA, 1997, Card 27-0051.
[14] Powder Diffraction File, Joint Committee on Powder Diffraction Standards, ASTM, Newtown Square, PA, 1997, Card 27-0050.
[15] Powder Diffraction File, Joint Committee on Powder Diffraction Standards, ASTM, Newtown Square, PA, 1997, Card 36-0287.
[16] Powder Diffraction File, Joint Committee on Powder Diffraction Standards, ASTM, Newtown Square, PA, 1997, Card 35-1007.
[17] P.G. Pai, S.S. Chao, Y. Takagi, G. Lucovsky, J. Vac. Sci. Technol., A, Vac. Surf. Films 4 (1986) 689.
[18] Z. Pan, D.O. Henderson, S.H. Morgan, J. Non-Cryst. Solids 171 (1994) 134.

[19] A.V. Khomich, Y.F. Kargin, P.I. Perov, V.M. Skorikov, Neorg. Mater. 26 (1990) 1709.
[20] O.M. Bordem, J. Appl. Spectrosc. 64 (1997) 476.
[21] F.L. Galeener, G. Lucovsky, Phys. Rev. Lett. 37 (1976) 1474.
[22] L. Leontie, M. Caraman, M. Alexe, C. Harnagea, Surf. Sci. 507/510 (2002) 480.
[23] M. Kobayashi, K. Harada, Y. Hirose, M. Ishii, I. Yamaga, Nucl. Instrum. Methods Phys. Res., A 400 (1997) 392.
[24] M. Yamaguchi, K. Hiraki, T. Nagatomo, Y. Masud, Jpn. J. Appl. Phys. 39 (2000) 5512.
[25] J.H. Kim, T. Tsurumi, T. Kamiya, M. Daimon, J. Appl. Phys. 75 (1994) 2924.